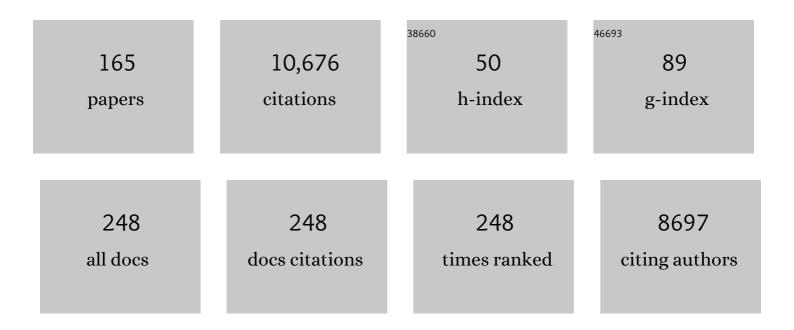
## K W Bowman

List of Publications by Year in descending order

Source: https://exaly.com/author-pdf/6539177/publications.pdf Version: 2024-02-01



K W ROWMAN

#	Article	IF	CITATIONS
1	Carbon monitoring system flux estimation and attribution: impact of ACOS-GOSAT XCO <sub>2</sub> sampling on the inference of terrestrial biospheric sources and sinks. Tellus, Series B: Chemical and Physical Meteorology, 2022, 66, 22486.	0.8	90
2	COVID-19 Lockdowns Afford the First Satellite-Based Confirmation That Vehicles Are an Under-recognized Source of Urban NH <sub>3</sub> Pollution in Los Angeles. Environmental Science and Technology Letters, 2022, 9, 3-9.	3.9	19
3	Attribution of Spaceâ€Time Variability in Globalâ€Ocean Dissolved Inorganic Carbon. Global Biogeochemical Cycles, 2022, 36, .	1.9	14
4	Changes in US background ozone associated with the 2011 turnaround in Chinese NOx emissions. Environmental Research Communications, 2022, 4, 045003.	0.9	1
5	Remotely Sensed Carbonyl Sulfide Constrains Model Estimates of Amazon Primary Productivity. Geophysical Research Letters, 2022, 49, .	1.5	7
6	Amazonian terrestrial water balance inferred from satellite-observed water vapor isotopes. Nature Communications, 2022, 13, 2686.	5.8	5
7	Top-down approaches. , 2022, , 87-155.		Ο
8	Satellite soil moisture data assimilation impacts on modeling weather variables and ozone in the southeastern US – Part 2: Sensitivity to dry-deposition parameterizations. Atmospheric Chemistry and Physics, 2022, 22, 7461-7487.	1.9	4
9	Satellite measurements of peroxyacetyl nitrate from the Cross-Track Infrared Sounder: comparison with ATom aircraft measurements. Atmospheric Measurement Techniques, 2022, 15, 3497-3511.	1.2	3
10	An assessment of emission characteristics of Northern Hemisphere cities using spaceborne observations of CO2, CO, and NO2. Remote Sensing of Environment, 2021, 254, 112246.	4.6	28
11	Carbon Monitoring System Flux Net Biosphere Exchange 2020 (CMS-Flux NBE 2020). Earth System Science Data, 2021, 13, 299-330.	3.7	40
12	Satellite Observations of the Tropical Terrestrial Carbon Balance and Interactions With the Water Cycle During the 21st Century. Reviews of Geophysics, 2021, 59, e2020RG000711.	9.0	13
13	2010–2015 North American methane emissions, sectoral contributions, and trends: a high-resolution inversion of GOSAT observations of atmospheric methane. Atmospheric Chemistry and Physics, 2021, 21, 4339-4356.	1.9	45
14	Air pollution trends measured from Terra: CO and AOD over industrial, fire-prone, and background regions. Remote Sensing of Environment, 2021, 256, 112275.	4.6	41
15	Global tropospheric ozone responses to reduced NO <sub> <i>x</i> </sub> emissions linked to the COVID-19 worldwide lockdowns. Science Advances, 2021, 7, .	4.7	72
16	Modeling the impact of COVID-19 on air quality in southern California: implications for future control policies. Atmospheric Chemistry and Physics, 2021, 21, 8693-8708.	1.9	26
17	Satellite soil moisture data assimilation impacts on modeling weather variables and ozone in the southeastern US – PartÂ1: An overview. Atmospheric Chemistry and Physics, 2021, 21, 11013-11040.	1.9	5
18	Changes in global terrestrial live biomass over the 21st century. Science Advances, 2021, 7, eabe9829.	4.7	136

#	Article	IF	CITATIONS
19	Covariation of Airborne Biogenic Tracers (CO <sub>2</sub> , COS, and CO) Supports Stronger Than Expected Growing Season Photosynthetic Uptake in the Southeastern US. Global Biogeochemical Cycles, 2021, 35, e2021GB006956.	1.9	7
20	A new methodology for inferring surface ozone from multispectral satellite measurements. Environmental Research Letters, 2021, 16, 105005.	2.2	6
21	The Atmospheric Carbon and Transport (ACT)-America Mission. Bulletin of the American Meteorological Society, 2021, 102, E1714-E1734.	1.7	17
22	Future Weakening of the ENSO Ocean Carbon Buffer Under Anthropogenic Forcing. Geophysical Research Letters, 2021, 48, e2021GL094021.	1.5	4
23	Emergent constraints on tropical atmospheric aridity—carbon feedbacks and the future of carbon sequestration. Environmental Research Letters, 2021, 16, 114008.	2.2	15
24	A Bayesian framework for deriving sector-based methane emissions from top-down fluxes. Communications Earth & Environment, 2021, 2, .	2.6	12
25	Societal shifts due to COVID-19 reveal large-scale complexities and feedbacks between atmospheric chemistry and climate change. Proceedings of the National Academy of Sciences of the United States of America, 2021, 118, .	3.3	42
26	The Carbon Cycle of Southeast Australia During 2019–2020: Drought, Fires, and Subsequent Recovery. AGU Advances, 2021, 2, .	2.3	21
27	Contrasting Regional Carbon Cycle Responses to Seasonal Climate Anomalies Across the Eastâ€West Divide of Temperate North America. Clobal Biogeochemical Cycles, 2020, 34, e2020CB006598.	1.9	12
28	Air Quality Response in China Linked to the 2019 Novel Coronavirus (COVIDâ€19) Lockdown. Geophysical Research Letters, 2020, 47, e2020GL089252.	1.5	74
29	The ECCOâ€Darwin Dataâ€Assimilative Global Ocean Biogeochemistry Model: Estimates of Seasonal to Multidecadal Surface Ocean <i>p</i> CO <sub>2</sub> and Airâ€Sea CO <sub>2</sub> Flux. Journal of Advances in Modeling Earth Systems, 2020, 12, e2019MS001888.	1.3	43
30	Atmospheric Simulations of Total Column CO2 Mole Fractions from Global to Mesoscale within the Carbon Monitoring System Flux Inversion Framework. Atmosphere, 2020, 11, 787.	1.0	11
31	Attribution of Chemistry-Climate Model Initiative (CCMI) ozone radiative flux bias from satellites. Atmospheric Chemistry and Physics, 2020, 20, 281-301.	1.9	6
32	Evaluation of a multi-model, multi-constituent assimilation framework for tropospheric chemical reanalysis. Atmospheric Chemistry and Physics, 2020, 20, 931-967.	1.9	40
33	Improved Constraints on Northern Extratropical CO <sub>2</sub> Fluxes Obtained by Combining Surfaceâ€Based and Spaceâ€Based Atmospheric CO <sub>2</sub> Measurements. Journal of Geophysical Research D: Atmospheres, 2020, 125, e2019JD032029.	1.2	26
34	Amplification of the Ocean Carbon Sink During El Niños: Role of Poleward Ekman Transport and Influence on Atmospheric CO <sub>2</sub> . Global Biogeochemical Cycles, 2020, 34, e2020GB006574.	1.9	27
35	Impacts of Degradation on Water, Energy, and Carbon Cycling of the Amazon Tropical Forests. Journal of Geophysical Research G: Biogeosciences, 2020, 125, e2020JG005677.	1.3	44
36	Carbon Flux Variability From a Relatively Simple Ecosystem Model With Assimilated Data Is Consistent With Terrestrial Biosphere Model Estimates. Journal of Advances in Modeling Earth Systems, 2020, 12, e2019MS001889.	1.3	22

#	Article	IF	CITATIONS
37	Fire decline in dry tropical ecosystems enhances decadal land carbon sink. Nature Communications, 2020, 11, 1900.	5.8	30
38	Comparison of optimal estimation HDOâ^•H <sub>2</sub> O retrievals from AIRS with ORACLES measurements. Atmospheric Measurement Techniques, 2020, 13, 1825-1834.	1.2	6
39	Lagged effects regulate the inter-annual variability of the tropical carbon balance. Biogeosciences, 2020, 17, 6393-6422.	1.3	26
40	Updated tropospheric chemistry reanalysis and emission estimates, TCR-2, for 2005–2018. Earth System Science Data, 2020, 12, 2223-2259.	3.7	54
41	Global distribution of methane emissions, emission trends, and OH concentrations and trends inferred from an inversion of GOSAT satellite data for 2010–2015. Atmospheric Chemistry and Physics, 2019, 19, 7859-7881.	1.9	111
42	Detection of fossil fuel emission trends in the presence of natural carbon cycle variability. Environmental Research Letters, 2019, 14, 084050.	2.2	8
43	Global satellite-driven estimates of heterotrophic respiration. Biogeosciences, 2019, 16, 2269-2284.	1.3	32
44	Characterization and evaluation of AIRS-based estimates of the deuterium content of water vapor. Atmospheric Measurement Techniques, 2019, 12, 2331-2339.	1.2	18
45	Flux towers in the sky: global ecology from space. New Phytologist, 2019, 224, 570-584.	3.5	111
46	Quantifying the Impact of Atmospheric Transport Uncertainty on CO <sub>2</sub> Surface Flux Estimates. Global Biogeochemical Cycles, 2019, 33, 484-500.	1.9	95
47	Balance of Emission and Dynamical Controls on Ozone During the Koreaâ€United States Air Quality Campaign From Multiconstituent Satellite Data Assimilation. Journal of Geophysical Research D: Atmospheres, 2019, 124, 387-413.	1.2	51
48	Detecting drought impact on terrestrial biosphere carbon fluxes over contiguous US with satellite observations. Environmental Research Letters, 2018, 13, 095003.	2.2	22
49	Retrievals of tropospheric ozone profiles from the synergism of AIRS and OMI: methodology and validation. Atmospheric Measurement Techniques, 2018, 11, 5587-5605.	1.2	43
50	A Hierarchical Statistical Framework for Emergent Constraints: Application to Snowâ€Albedo Feedback. Geophysical Research Letters, 2018, 45, 13,050.	1.5	30
51	Response to Comment on "Contrasting carbon cycle responses of the tropical continents to the 2015–2016 El Niño― Science, 2018, 362, .	6.0	6
52	The Tropospheric Emission Spectrometer: From Discovery Mission to Earth System Sounding. , 2018, , .		0
53	Contrasting carbon cycle responses of the tropical continents to the 2015–2016 El Niño. Science, 2017, 358, .	6.0	307
54	Global and Brazilian Carbon Response to El Niño Modoki 2011–2010. Earth and Space Science, 2017, 4, 637-660.	1.1	49

#	Article	IF	CITATIONS
55	Evaluation of ACCMIP ozone simulations and ozonesonde sampling biases using a satellite-based multi-constituent chemical reanalysis. Atmospheric Chemistry and Physics, 2017, 17, 8285-8312.	1.9	15
56	Impact of intercontinental pollution transport on North American ozone air pollution: an HTAP phase 2 multi-model study. Atmospheric Chemistry and Physics, 2017, 17, 5721-5750.	1.9	51
57	Seasonal and spatial changes in trace gases over megacities from Aura TES observations: two case studies. Atmospheric Chemistry and Physics, 2017, 17, 9379-9398.	1.9	8
58	Decadal changes in global surface NO <sub><i>x</i></sub> emissions from multi-constituent satellite data assimilation. Atmospheric Chemistry and Physics, 2017, 17, 807-837.	1.9	228
59	A global wetland methane emissions and uncertainty dataset for atmospheric chemical transport models (WetCHARTs version 1.0). Geoscientific Model Development, 2017, 10, 2141-2156.	1.3	161
60	Evaluation and attribution of OCO-2 XCO <sub>2</sub> uncertainties. Atmospheric Measurement Techniques, 2017, 10, 2759-2771.	1.2	39
61	Hydrological controls on the tropospheric ozone greenhouse gas effect. Elementa, 2017, 5, .	1.1	5
62	High-resolution tropospheric carbon monoxide profiles retrieved from CrIS and TROPOMI. Atmospheric Measurement Techniques, 2016, 9, 2567-2579.	1.2	46
63	A method for independent validation of surface fluxes from atmospheric inversion: Application to CO 2. Geophysical Research Letters, 2016, 43, 3502-3508.	1.5	10
64	Comparison between the Local Ensemble Transform Kalman Filter (LETKF) and 4Dâ€Var in atmospheric CO <sub>2</sub> flux inversion with the Goddard Earth Observing Systemâ€Chem model and the observation impact diagnostics from the LETKF. Journal of Geophysical Research D: Atmospheres, 2016, 121, 13,066.	1.2	19
65	Satellite observations of ethylene (C2H4) from the Aura Tropospheric Emission Spectrometer: A scoping study. Atmospheric Environment, 2016, 141, 388-393.	1.9	6
66	Gridded National Inventory of U.S. Methane Emissions. Environmental Science & Technology, 2016, 50, 13123-13133.	4.6	165
67	A recycling method for the large-eddy simulation of plumes in the atmospheric boundary layer. Environmental Fluid Mechanics, 2016, 16, 69-85.	0.7	18
68	Improved western U.S. background ozone estimates via constraining nonlocal and local source contributions using Aura TES and OMI observations. Journal of Geophysical Research D: Atmospheres, 2015, 120, 3572-3592.	1.2	15
69	Assessing the magnitude of CO <sub>2</sub> flux uncertainty in atmospheric CO <sub>2</sub> records using products from NASA's Carbon Monitoring Flux Pilot Project. Journal of Geophysical Research D: Atmospheres, 2015, 120, 734-765.	1.2	41
70	Improved analysisâ€error covariance matrix for highâ€dimensional variational inversions: application to source estimation using a 3D atmospheric transport model. Quarterly Journal of the Royal Meteorological Society, 2015, 141, 1906-1921.	1.0	48
71	Toward "optimal―integration of terrestrial biosphere models. Geophysical Research Letters, 2015, 42, 4418-4428.	1.5	48
72	Estimate of carbonyl sulfide tropical oceanic surface fluxes using Aura Tropospheric Emission Spectrometer observations. Journal of Geophysical Research D: Atmospheres, 2015, 120, 11,012.	1.2	43

#	Article	IF	CITATIONS
73	Sensitivity analysis of the potential impact of discrepancies in stratosphere–troposphere exchange on inferred sources and sinks of CO <sub>2</sub> . Atmospheric Chemistry and Physics, 2015, 15, 11773-11788.	1.9	19
74	Influence of ENSO and the NAO on terrestrial carbon uptake in the Texasâ€northern Mexico region. Global Biogeochemical Cycles, 2015, 29, 1247-1265.	1.9	29
75	The impact of observing characteristics on the ability to predict ozone under varying polluted photochemical regimes. Atmospheric Chemistry and Physics, 2015, 15, 10645-10667.	1.9	6
76	Instantaneous longwave radiative impact of ozone: an application on IASI/MetOp observations. Atmospheric Chemistry and Physics, 2015, 15, 12971-12987.	1.9	14
77	Estimating global and North American methane emissions with high spatial resolution using GOSAT satellite data. Atmospheric Chemistry and Physics, 2015, 15, 7049-7069.	1.9	225
78	Quantifying lower tropospheric methane concentrations using GOSAT near-IR and TES thermal IR measurements. Atmospheric Measurement Techniques, 2015, 8, 3433-3445.	1.2	34
79	Sourceâ€receptor relationships of columnâ€average CO <sub>2</sub> and implications for the impact of observations on flux inversions. Journal of Geophysical Research D: Atmospheres, 2015, 120, 5214-5236.	1.2	22
80	Using Green's Functions to initialize and adjust a global, eddying ocean biogeochemistry general circulation model. Ocean Modelling, 2015, 95, 1-14.	1.0	22
81	Rapid increases in tropospheric ozone production and export from China. Nature Geoscience, 2015, 8, 690-695.	5.4	256
82	Changes in nitrogen oxides emissions in California during 2005–2010 indicated from topâ€down and bottomâ€up emission estimates. Journal of Geophysical Research D: Atmospheres, 2014, 119, 12,928.	1.2	16
83	Terrestrial gross primary production inferred from satellite fluorescence and vegetation models. Global Change Biology, 2014, 20, 3103-3121.	4.2	161
84	Assessment of source contributions to seasonal vegetative exposure to ozone in the U.S Journal of Geophysical Research D: Atmospheres, 2014, 119, 324-340.	1.2	43
85	The Atmospheric Infrared Sounder version 6 cloud products. Atmospheric Chemistry and Physics, 2014, 14, 399-426.	1.9	99
86	Inferring regional sources and sinks of atmospheric CO <sub>2</sub> from GOSAT XCO <sub>2</sub> data. Atmospheric Chemistry and Physics, 2014, 14, 3703-3727.	1.9	120
87	Toward the next generation of air quality monitoring: Ozone. Atmospheric Environment, 2013, 80, 571-583.	1.9	48
88	Interpreting seasonal changes in the carbon balance of southern Amazonia using measurements of XCO <sub>2</sub> and chlorophyll fluorescence from GOSAT. Geophysical Research Letters, 2013, 40, 2829-2833.	1.5	89
89	Attribution of historical ozone forcing to anthropogenic emissions. Nature Climate Change, 2013, 3, 567-570.	8.1	42
90	Achieving Climate Change Absolute Accuracy in Orbit. Bulletin of the American Meteorological Society, 2013, 94, 1519-1539.	1.7	239

#	Article	IF	CITATIONS
91	Validation of six years of TES tropospheric ozone retrievals with ozonesonde measurements: implications for spatial patterns and temporal stability in the bias. Atmospheric Measurement Techniques, 2013, 6, 1413-1423.	1.2	39
92	Decadal record of satellite carbon monoxide observations. Atmospheric Chemistry and Physics, 2013, 13, 837-850.	1.9	207
93	Profiling tropospheric CO <sub>2</sub> using Aura TES and TCCON instruments. Atmospheric Measurement Techniques, 2013, 6, 63-79.	1.2	17
94	A Practical Method to Estimate Information Content in the Context of 4D-Var Data Assimilation. SIAM-ASA Journal on Uncertainty Quantification, 2013, 1, 106-138.	1.1	13
95	Pre-industrial to end 21st century projections of tropospheric ozone from the Atmospheric Chemistry and Climate Model Intercomparison Project (ACCMIP). Atmospheric Chemistry and Physics, 2013, 13, 2063-2090.	1.9	570
96	Characterization of ozone profiles derived from Aura TES and OMI radiances. Atmospheric Chemistry and Physics, 2013, 13, 3445-3462.	1.9	74
97	CH <sub>4</sub> and CO distributions over tropical fires during October 2006 as observed by the Aura TES satellite instrument and modeled by GEOS-Chem. Atmospheric Chemistry and Physics, 2013, 13, 3679-3692.	1.9	39
98	Tropospheric ozone changes, radiative forcing and attribution to emissions in the Atmospheric Chemistry and Climate Model Intercomparison Project (ACCMIP). Atmospheric Chemistry and Physics, 2013, 13, 3063-3085.	1.9	361
99	Interactive ozone and methane chemistry in GISS-E2 historical and future climate simulations. Atmospheric Chemistry and Physics, 2013, 13, 2653-2689.	1.9	150
100	Impacts of transported background pollutants on summertime western US air quality: model evaluation, sensitivity analysis and data assimilation. Atmospheric Chemistry and Physics, 2013, 13, 359-391.	1.9	28
101	Evaluation of ACCMIP outgoing longwave radiation from tropospheric ozone using TES satellite observations. Atmospheric Chemistry and Physics, 2013, 13, 4057-4072.	1.9	61
102	El Niño, the 2006 Indonesian peat fires, and the distribution of atmospheric methane. Geophysical Research Letters, 2013, 40, 4938-4943.	1.5	40
103	Impact of model errors in convective transport on CO source estimates inferred from MOPITT CO retrievals. Journal of Geophysical Research D: Atmospheres, 2013, 118, 2073-2083.	1.2	62
104	Carbon monoxide (CO) vertical profiles derived from joined TES and MLS measurements. Journal of Geophysical Research D: Atmospheres, 2013, 118, 10,601.	1.2	12
105	Impact of Southern California anthropogenic emissions on ozone pollution in the mountain states: Model analysis and observational evidence from space. Journal of Geophysical Research D: Atmospheres, 2013, 118, 12,784.	1.2	21
106	Profiles of CH <sub>4</sub> , HDO, H <sub>2</sub> O, and N <sub>2</sub> O with improved lower tropospheric vertical resolution from Aura TES radiances. Atmospheric Measurement Techniques, 2012, 5, 397-411.	1.2	141
107	The influence of boreal biomass burning emissions on the distribution of tropospheric ozone over North America and the North Atlantic during 2010. Atmospheric Chemistry and Physics, 2012, 12, 2077-2098.	1.9	90
108	A multi-sensor upper tropospheric ozone product (MUTOP) based on TES ozone and GOES water vapor: validation with ozonesondes. Atmospheric Chemistry and Physics, 2012, 12, 5661-5676.	1.9	4

#	Article	IF	CITATIONS
109	Impacts of midlatitude precursor emissions and local photochemistry on ozone abundances in the Arctic. Journal of Geophysical Research, 2012, 117, .	3.3	55
110	Attribution of direct ozone radiative forcing to spatially resolved emissions. Geophysical Research Letters, 2012, 39, .	1.5	35
111	Information Theoretic Metrics to Characterize Observations in Variational Data Assimilation. Procedia Computer Science, 2012, 9, 1047-1055.	1.2	4
112	The vertical distribution of ozone instantaneous radiative forcing from satellite and chemistry climate models. Journal of Geophysical Research, 2011, 116, .	3.3	40
113	Sensitivity of outgoing longwave radiative flux to the global vertical distribution of ozone characterized by instantaneous radiative kernels from Aura-TES. Journal of Geophysical Research, 2011, 116, .	3.3	36
114	Inverse modeling of CO <sub>2</sub> sources and sinks using satellite observations of CO <sub>2</sub> from TES and surface flask measurements. Atmospheric Chemistry and Physics, 2011, 11, 6029-6047.	1.9	94
115	Estimate of bias in Aura TES HDO/H <sub>2</sub> 0 profiles from comparison of TES and in situ HDO/H <sub>2</sub> 0 measurements at the Mauna Loa observatory. Atmospheric Chemistry and Physics, 2011, 11, 4491-4503.	1.9	59
116	The impact of orbital sampling, monthly averaging and vertical resolution on climate chemistry model evaluation with satellite observations. Atmospheric Chemistry and Physics, 2011, 11, 6493-6514.	1.9	31
117	A multi-sensor upper tropospheric ozone product (MUTOP) based on TES Ozone and GOES water vapor: derivation. Atmospheric Chemistry and Physics, 2011, 11, 6515-6527.	1.9	5
118	Relating tropical ocean clouds to moist processes using water vapor isotope measurements. Atmospheric Chemistry and Physics, 2011, 11, 741-752.	1.9	45
119	Global multi-year O <sub>3</sub> -CO correlation patterns from models and TES satellite observations. Atmospheric Chemistry and Physics, 2011, 11, 5819-5838.	1.9	54
120	Construction of non-diagonal background error covariance matrices for global chemical data assimilation. Geoscientific Model Development, 2011, 4, 299-316.	1.3	46
121	Validation of northern latitude Tropospheric Emission Spectrometer stare ozone profiles with ARC-IONS sondes during ARCTAS: sensitivity, bias and error analysis. Atmospheric Chemistry and Physics, 2010, 10, 9901-9914.	1.9	58
122	Characterization of Tropospheric Emission Spectrometer (TES) CO <sub>2</sub> for carbon cycle science. Atmospheric Chemistry and Physics, 2010, 10, 5601-5623.	1.9	100
123	Modeling global atmospheric CO <sub>2</sub> with improved emission inventories and CO <sub>2</sub> production from the oxidation of other carbon species. Geoscientific Model Development, 2010, 3, 689-716.	1.3	117
124	Implementation and evaluation of an array of chemical solvers in the Global Chemical Transport Model GEOS-Chem. Geoscientific Model Development, 2009, 2, 89-96.	1.3	23
125	Atmospheric sounding simulation experiment service. , 2009, , .		0
126	Ozone production in boreal fire smoke plumes using observations from the Tropospheric Emission Spectrometer and the Ozone Monitoring Instrument. Journal of Geophysical Research, 2009, 114, .	3.3	48

#	Article	IF	CITATIONS
127	Observed vertical distribution of tropospheric ozone during the Asian summertime monsoon. Journal of Geophysical Research, 2009, 114, .	3.3	59
128	Impacts of background ozone production on Houston and Dallas, Texas, air quality during the Second Texas Air Quality Study field mission. Journal of Geophysical Research, 2009, 114, .	3.3	45
129	Impact of the assimilation of ozone from the Tropospheric Emission Spectrometer on surface ozone across North America. Geophysical Research Letters, 2009, 36, .	1.5	49
130	The zonal structure of tropical O <sub>3</sub> and CO as observed by the Tropospheric Emission Spectrometer in November 2004 – Part 1: Inverse modeling of CO emissions. Atmospheric Chemistry and Physics, 2009, 9, 3547-3562.	1.9	67
131	The zonal structure of tropical O <sub>3</sub> and CO as observed by the Tropospheric Emission Spectrometer in November 2004 – Part 2: Impact of surface emissions on O <sub>3</sub> and its precursors. Atmospheric Chemistry and Physics, 2009. 9. 3563-3582.	1.9	25
132	Improving GEOS-Chem Model Tropospheric Ozone through Assimilation of Pseudo Tropospheric Emission Spectrometer Profile Retrievals. Lecture Notes in Computer Science, 2009, , 302-311.	1.0	3
133	Satellite measurements of the clear-sky greenhouse effect from tropospheric ozone. Nature Geoscience, 2008, 1, 305-308.	5.4	84
134	Effects of the 2006 El Niño on tropospheric composition as revealed by data from the Tropospheric Emission Spectrometer (TES). Geophysical Research Letters, 2008, 35, .	1.5	113
135	Validation of Tropospheric Emission Spectrometer (TES) measurements of the total, stratospheric, and tropospheric column abundance of ozone. Journal of Geophysical Research, 2008, 113, .	3.3	80
136	Validation of Tropospheric Emission Spectrometer (TES) nadir ozone profiles using ozonesonde measurements. Journal of Geophysical Research, 2008, 113, .	3.3	181
137	Comparison of Tropospheric Emission Spectrometer nadir water vapor retrievals with in situ measurements. Journal of Geophysical Research, 2008, 113, .	3.3	38
138	Tropospheric Emission Spectrometer nadir spectral radiance comparisons. Journal of Geophysical Research, 2008, 113, .	3.3	38
139	Implementation of cloud retrievals for TES atmospheric retrievals: 2. Characterization of cloud top pressure and effective optical depth retrievals. Journal of Geophysical Research, 2008, 113, .	3.3	50
140	Estimating the summertime tropospheric ozone distribution over North America through assimilation of observations from the Tropospheric Emission Spectrometer. Journal of Geophysical Research, 2008, 113, .	3.3	87
141	First satellite observations of lower tropospheric ammonia and methanol. Geophysical Research Letters, 2008, 35, .	1.5	111
142	Measurements of SO <sub>2</sub> profiles in volcanic plumes from the NASA Tropospheric Emission Spectrometer (TES). Geophysical Research Letters, 2008, 35, .	1.5	37
143	Sensor-web Operations Explorer (SOX) for Earth Science Air Quality Mission Concepts. Aerospace Conference Proceedings IEEE, 2008, , .	0.0	1
144	Remote Sensing of Tropospheric Pollution from Space. Bulletin of the American Meteorological Society, 2008, 89, 805-822.	1.7	108

#	Article	IF	CITATIONS
145	Impact of nonlinearity on changing the a priori of trace gas profile estimates from the Tropospheric Emission Spectrometer (TES). Atmospheric Chemistry and Physics, 2008, 8, 3081-3092.	1.9	29
146	Transpacific transport of ozone pollution and the effect of recent Asian emission increases on air quality in North America: an integrated analysis using satellite, aircraft, ozonesonde, and surface observations. Atmospheric Chemistry and Physics, 2008, 8, 6117-6136.	1.9	369
147	Improved tropospheric ozone profile retrievals using OMI and TES radiances. Geophysical Research Letters, 2007, 34, .	1.5	85
148	Tropospheric vertical distribution of tropical Atlantic ozone observed by TES during the northern African biomass burning season. Geophysical Research Letters, 2007, 34, .	1.5	71
149	Comparisons of Tropospheric Emission Spectrometer (TES) ozone profiles to ozonesondes: Methods and initial results. Journal of Geophysical Research, 2007, 112, .	3.3	184
150	Importance of rain evaporation and continental convection in the tropical water cycle. Nature, 2007, 445, 528-532.	13.7	401
151	Tropospheric Emission Spectrometer observations of the tropospheric HDO/H2O ratio: Estimation approach and characterization. Journal of Geophysical Research, 2006, 111, .	3.3	167
152	Implementation of cloud retrievals for Tropospheric Emission Spectrometer (TES) atmospheric retrievals: part 1. Description and characterization of errors on trace gas retrievals. Journal of Geophysical Research, 2006, 111, .	3.3	107
153	Ozone-CO correlations determined by the TES satellite instrument in continental outflow regions. Geophysical Research Letters, 2006, 33, n/a-n/a.	1.5	92
154	Forward model and Jacobians for Tropospheric Emission Spectrometer retrievals. IEEE Transactions on Geoscience and Remote Sensing, 2006, 44, 1308-1323.	2.7	84
155	TES level 1 algorithms: interferogram processing, geolocation, radiometric, and spectral calibration. IEEE Transactions on Geoscience and Remote Sensing, 2006, 44, 1288-1296.	2.7	31
156	Calculation of altitude-dependent tikhonov constraints for TES nadir retrievals. IEEE Transactions on Geoscience and Remote Sensing, 2006, 44, 1334-1342.	2.7	57
157	TES atmospheric profile retrieval characterization: an orbit of simulated observations. IEEE Transactions on Geoscience and Remote Sensing, 2006, 44, 1324-1333.	2.7	43
158	Two-dimensional characterization of atmospheric profile retrievals from limb sounding observations. Journal of Quantitative Spectroscopy and Radiative Transfer, 2004, 86, 45-71.	1.1	25
159	Predicted errors of tropospheric emission spectrometer nadir retrievals from spectral window selection. Journal of Geophysical Research, 2004, 109, .	3.3	165
160	Potential of observations from the Tropospheric Emission Spectrometer to constrain continental sources of carbon monoxide. Journal of Geophysical Research, 2003, 108, n/a-n/a.	3.3	77
161	Application of a nonuniform spectral resampling transform in Fourier-transform spectrometry. Applied Optics, 2003, 42, 1122.	2.1	8
162	Capturing time and vertical variability of tropospheric ozone: A study using TES nadir retrievals. Journal of Geophysical Research, 2002, 107, ACH 21-1-ACH 21-11.	3.3	87

#	Article	IF	CITATIONS
163	Farâ€Ultraviolet Intensities and Centerâ€toâ€Limb Variations of Active Regions and Quiet Sun UsingUARSSOLSTICE Irradiance Measurements and Groundâ€based Spectroheliograms. Astrophysical Journal, 2001, 560, 1020-1034.	1.6	21
164	Instrument line-shape modeling and correction for off-axis detectors in Fourier-transform spectrometry. Applied Optics, 2000, 39, 3765.	2.1	19
165	<title>Wavelet analysis of random fields and multiresolution Wiener filtering</title> . , 1995, , .		2